Princeton Plasma Physics Laboratory

PPPL- 4612

PPPL- 4612

Large Area Divertor Temperature Measurements Using A High-speed Camera With Near-infraed Fiters in NSTX

B.C. Lyons, F. Scotti, S.J. Zweben, T.K. Gray, J. Hosea, R. Kaita, H.W. Kugel, R.J. Maqueda, A.G. McLean, A.L. Roquemore, V.A. Soukhanovskii and G. Taylor

April, 2011

Prepared for the U.S. Department of Energy under Contract DE-AC02-09CH11466.

Princeton Plasma Physics Laboratory
Report Disclaimers

Full Legal Disclaimer

Trademark Disclaimer

PPPL Report Availability

Princeton Plasma Physics Laboratory:

http://www.pppl.gov/techreports.cfm

Office of Scientific and Technical Information (OSTI):

http://www.osti.gov/bridge

Related Links:

U.S. Department of Energy

Office of Scientific and Technical Information

Fusion Links

Large area divertor temperature measurements using a high-speed camera with near-infrared filters in NSTX

B.C. Lyons,[1] F. Scotti,[1] S.J. Zweben,[1] T.K. Gray,[2] J. Hosea,[1] R. Kaita,[1] H.W. Kugel,[1] R.J. Maqueda,[1] A.G. McLean,[2] A.L. Roquemore,[1] V.A. Soukhanovskii,[3] and G. Taylor[1]

[1)] *Princeton Plasma Physics Laboratory, Princeton, NJ 08543*

[2)] *Oak Ridge National Laboratory, Oak Ridge, TN 37831*

[3)] *Lawrence Livermore National Laboratory, Livermore, CA 94550*

(Dated: 30 March 2011)

Fast cameras already installed on the National Spherical Torus Experiment (NSTX) have be equipped with near-infrared (NIR) filters in order to measure the surface temperature in the lower divertor region. Such a system provides a unique combination of high speed (> 50 kHz) and wide field-of-view ($> 50\%$ of the divertor). Benchtop calibrations demonstrated the system's ability to measure thermal emission down to 330 ^{o}C. There is also, however, significant plasma light background in NSTX. Without improvements in background reduction, the current system is incapable of measuring signals below the background equivalent temperature (600 - 700 ^{o}C). Thermal signatures have been detected in cases of extreme divertor heating. It is observed that the divertor can reach temperatures around 800 ^{o}C when high harmonic fast wave (HHFW) heating is used. These temperature profiles were fit using a simple heat diffusion code, providing a measurement of the heat flux to the divertor. Comparisons to other infrared thermography systems on NSTX are made.

I. INTRODUCTION

In recent years it has become of critical importance to the nuclear fusion research community to manage the intense particle and heat fluxes intrinsic to modern and next-generation high performance tokamaks, particularly in the divertor region. While divertor geometry and active techniques can be used to help mitigate these fluxes, plasma facing components (PFCs) must still be made of materials that can withstand continuous heat loads of 10 - 20 MW/m^2. Transient heat loads from ELMs and disruptions can be much higher. Most commonly, carbon-based materials (like graphite or carbon fiber composite) or high-Z materials (like tungsten or molybdenum) are used for this application. The ITER divertor will use a combination of both of these materials[1,2].

It is necessary for researchers to monitor the temperature of PFCs in real time to prevent the sublimation and erosion of carbon-based materials and the melting of high-Z materials. For this purpose, nearly all large-scale tokamaks employ infrared (IR) cameras. Among the projects currently using IR thermography are ASDEX Upgrade[3,4], JET[5–8], MAST[9], TCV[10], and Alcator C-Mod[11]. Furthermore, an IR thermography system will be present on ITER[12]. These cameras have a variety of sensitivity bands in the range of 1.5 - 10 μm. In addition, they have varying maximum frame rates from tens of Hz to tens of kHz. Often, researchers must face a trade-off between large fields of view (for effective monitoring of divertor hot spot development) and fast frame rates (for studying transient events in real time).

The National Spherical Torus Experiment (NSTX) has several IR cameras installed which are operated by the Oak Ridge National Laboratory (ORNL). One slow (30 Hz) IR camera monitors the lower divertor while another monitors the upper divertor. Each camera has a sensitivity band of 7 - 13 μm[13]. An approximate field of view for the the lower divertor camera can be seen as the blue box in Figure 1a. In addition, a fast (1.6 - 6.3 kHz) IR camera has been installed[14]. This originally had a sensitivity band of 8 - 10 μm. Recently, this camera was converted to a dual-band system, with bands from 4 - 6 μm and 7 - 10 μm[15]. The field of view of this camera is rotatable and is shown as the green and red boxes in Figure 1a.

In this paper, we describe a technique to measure the surface temperature of the NSTX divertor plates over a large area using high-speed cameras with NIR filters. In particular, we are interested in developing an IR thermography system that effectively monitors the NSTX divertor for hot spot development over a wider area than currently possible and at a high enough speed to monitor transient events. Two Vision Research Phantom cameras already installed on NSTX have fields of view (see Figure 1) of greater than half of the NSTX divertor and frame rates at full field of view of at least 50 kHz. While these cameras are mainly sensitive to visible light, their spectral responsivities extend into the near-infrared (NIR). It has been noted previously that plasma line emission and bremmstralung radiation could potentially dominate the NIR light within NSTX[16]. At high enough temperatures, however, it is expected that thermal blackbody radiation from the divertor would dominate in this range.

Section II describes NSTX and our experimental setup in greater detail. Section III A discusses the background equivalent temperature due to plasma light found under normal NSTX operation. In Section III B, we demonstrate our systems' ability to measure the temperature of hot spots formed during RF heating of the plasma. Finally, Section IV summarizes our results and provides areas for future research.

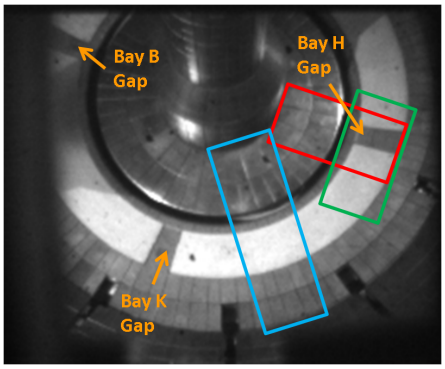

(a) Phantom v7.3 view from Bay J. The ORNL slow IR camera (blue)[14] and fast, dual-band IR camera radial (red) and toroidal (green)[15] views are superimposed.

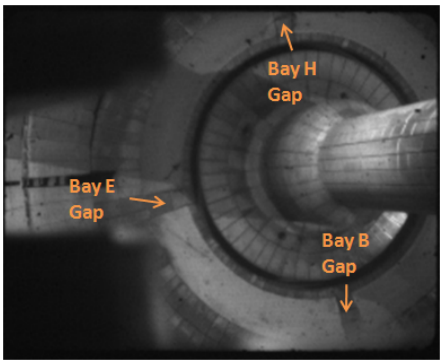

(b) Phantom v710 view from Bay E

FIG. 1: View of NSTX lower divertor from the fast cameras. The four gaps of the LLD are labeled, demonstrating complete coverage of the lower divertor. The width of each LLD plate is 20 cm.

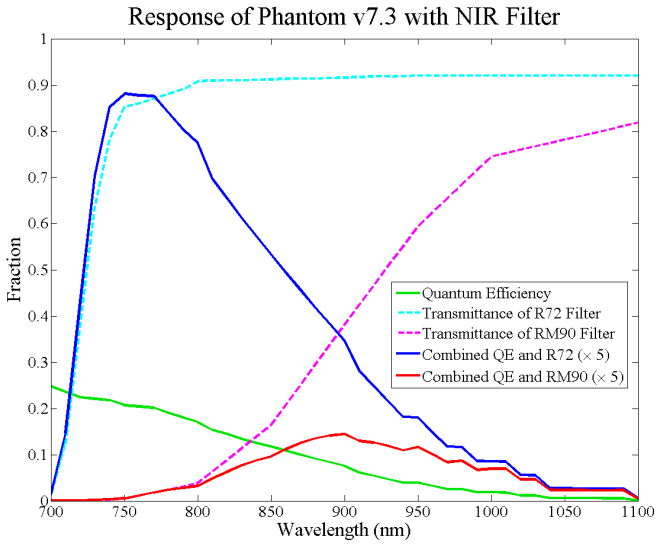

FIG. 2: The response of the Phantom v7.3 camera with NIR filters vs wavelength. The low transmittance of the filters at short wavelengths and the low responsivity of the camera at high wavelengths creates an effective NIR bandpass system.

II. EXPERIMENTAL SETUP AND PROCEDURE

NSTX is a DOE National User Facility used to study the magnetic confinement of plasmas in a medium-scale, low aspect ratio torus. It operates as a pulsed device with each plasma shot lasting on the order of one second.

There are twelve diagnostic bays (labeled A through L) spaced out every 30^o toroidally around NSTX, allowing for a wide variety of measurements to be taken for every plasma shot. We have mounted two Vision Research high-speed cameras with wide-angle views of the lower divertor. Together, the Phantom v7.3 located at Bay J and the Phantom v710 located at Bay E provide complete coverage of the Liquid Lithium Divertor (LLD) and near-complete coverage of the entire lower divertor (see Figure 1). The v7.3 is capable of frame rates up to $\sim$ 50 kHz at the 224x184 resolution typically used, while the v710 is capable of frame rates up to $\sim$ 100 kHz with a 256x208 resolution. Both cameras allow a minimum exposure time of 1 μs. The v7.3 has a maximum exposure of 99 ms while the v710's is 41 ms.

For the present application, both cameras were equipped with both Hoya R72 ($>$ 720 nm) and Hoya RM90 ($>$ 900 nm) cutoff filters. A filter wheel system allows the user to easily switch between either IR filter (or several other emission line bandpass filters) from shot to shot. As the Phantom cameras are mainly intended for visible light applications, the spectral responsivity of both cameras rapidly approaches zero around 1100 nm; this, along with the IR cutoff filters, effectively makes a high-speed, NIR-bandpass camera system (e.g., see Figure 2 for the v7.3 system's response). A benchtop calibration with a blackbody source was performed for both cameras with the 720 nm filter from 330 ^{o}C to 670 ^{o}C. A good exponential fit was made to both camera's calibration curves allowing for easy conversion between pixel count and temperature as well as extrapolation above 670 ^{o}C. The e-folding temperature of these calibration curves matched to within a few percent of those theoretically predicted by passing a blackbody curve through the optical components of our system. The overall coefficient on the exponentials matched to within a few tens of percent, depending on certain assumptions that are made. Currently, the calibration curves are corrected for the 900 nm filter using blackbody theory, though a benchtop calibration to confirm the modified curves is planned for the near future. In addition, blackbody theory could be used to more accurately extrapolate our calibration curves, though this has not yet been done. Furthermore, as conditions within the spherical torus are constantly changing throughout the run, we have not attempted to correct for any *in situ* effects (e.g., coatings on the camera windows or non-ideal emissivities).

Data has been recorded for about 100 shots with a variety of plasma conditions over the course several months..

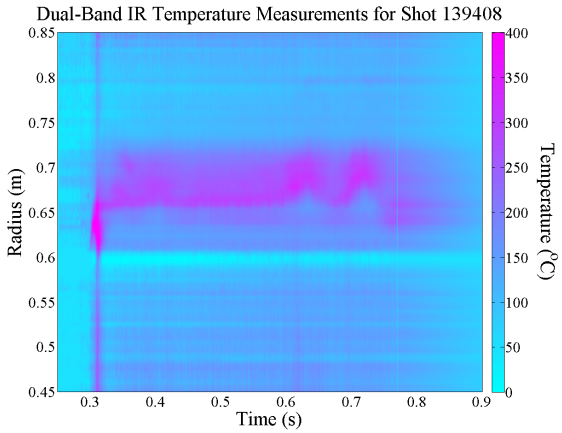

(a) Temperature inferred from ORNL dual-band camera data

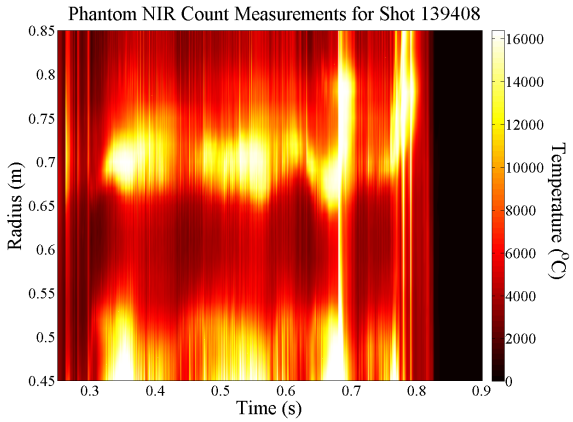

(b) Counts measured by Bay J camera w/ 900 nm filter and 990 μs exposure time

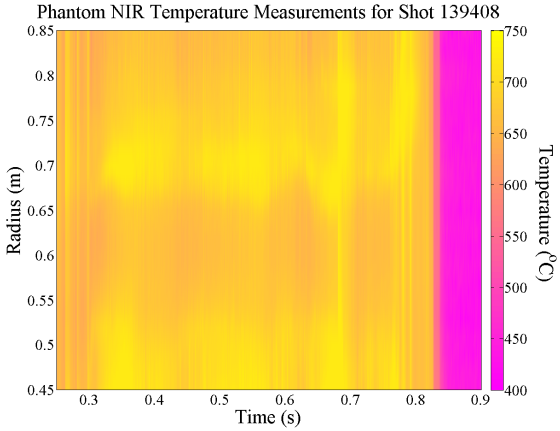

(c) Temperature inferred from Bay J camera w/ 900 nm filter and 990 μs exposure time. This is created by normalizing the counts in Figure 3b to the calibration exposure time and then converting to temperature using the calibration curve.

FIG. 3: Camera data from the lower divertor near Bay H versus radius and time for shot 139408. Note that pink corresponds to the same temperature (400 ^{o}C) in Figures 3a and 3c. As explained in Section III A, the temperature inferred from the Phantom camera data (Figure 3c) appears much too high and the counts measured (Figure 3b) are attributed mainly to background plasma line emission.

III. DATA ANALYSIS

A. Magnitude of background under typical operating parameters

In order to evaluate the effectiveness of our camera system *in situ*, we have compared data taken with our system for shot 139408 to data for the same shot from the ORNL dual-band fast IR camera. This 0.83 ms shot had an 800 kA toroidal current, a 4.7 kG toroidal magnetic field, and 4 MW of neutral beam heating. As noted in Figure 1a, the dual-band camera's field of view is restricted to the area inside the red box near Bay H. This extends from about 0.25 m to 0.85 m radially and approximately 15^o toroidally. Figure 3a shows the temperatures measured by the ORNL camera versus radius and time. The outer strike point, which was held fixed on the Liquid Lithium Divertor (LLD) between 0.65 m and 0.85 m is clearly visible, with a measured temperature of $\sim$ 350 ^{o}C. Elsewhere on the divertor, there is an ambient temperature between 100 ^{o}C and 200 ^{o}C, with the exception of the region located around 0.6 m. This is the coaxial helicity injection (CHI) gap where there is a hole in the divertor; as one would expect, the temperature in this region is near zero. Temporally, we see that the temperature stays roughly constant at a given radius during the shot, except when the strike point moves (e.g., between 0.6 s and 0.75 s). When the shot ends just after 0.8 s, we see that the temperature of the divertor decreases slowly and steadily, dropping several hundred degrees over the course of 100 ms.

To compare to the ORNL camera data, we looked at the data from the Phantom v7.3 camera contained inside

the red box of Figure 1a. The counts recorded (averaged toroidally across the red box) are shown in Figure 3b. In excess of 10,000 counts are measured around the strike point between 0.65 m and 0.85 m. We also see a similarly large number of counts on the inner divertor between 0.45 m and 0.55 m. The area of the CHI gap is dimmer, though over a thousand counts are still recorded. After the shot ends, the counts drop rapidly to near zero everywhere. The temperature inferred by these counts given our calibration is shown in Figure 3c. Note that pink corresponds to 400 ^{o}C in both Figures 3a and 3c. Clearly, the temperatures inferred from the Phantom camera data are universally several hundred degrees hotter than those measured by the ORNL camera. In the area of the strike point, the observed temperature is $\sim$ 700 ^{o}C, while it decreases to around 600 ^{o}C elsewhere, even in the CHI gap. Furthermore, at the end of the shot, the temperature decreases rapidly, falling to about 400 ^{o}C at every radius in the span of about 10 ms.

All of these discrepancies between the two cameras' measurements can be explained by a high level of background plasma light in the Phantom camera's measurements that is not detectable by the ORNL camera. Firstly, the temperatures measured by the ORNL camera are well-below or just at the minimum temperature that would be visible to the Phantom v7.3 camera with the 900 nm filter and 990 μs exposure time. Thus, we would expect thermal emission to provide no more than around 100 counts. The system, however, records thousands and tens of thousands of counts. A high level background plasma light would greatly increase the observed counts and thus the observed temperature given such a low level of thermal emission. The strike point would be brightest in plasma light, explaining our ability to see the strike point with the Phantom camera system despite the low temperature measured by the ORNL camera. In addition, the region around the CHI gap would still have low but non-negligible levels of plasma light despite the hole in the divertor there. Lastly, the plasma light would abruptly disappear at the end of the shot, leading to an abrupt decrease in the measured temperature, as is observed. Thus, during a shot there appears to be a background equivalent temperature between 600 ^{o}C and 700 ^{o}C, likely due to NIR line emission from the plasma. When the shot ends, there is only a little background remaining likely due to the reflection of light from a filament used to assist in the initial breakdown in the plasma and the irreducible small number of counts that the camera reports even in total darkness. This creates a background equivalent temperature of approximately 400 ^{o}C. During a shot, therefore, it is likely impossible to measure temperatures much below $\sim$ 700 ^{o}C with the current system due to background light, despite the minimum observable temperature of 330 ^{o}C in the calibration.

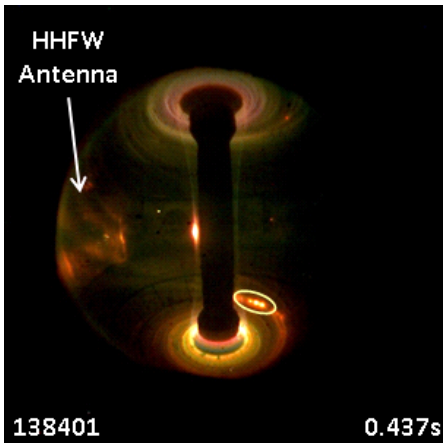

(a) Bay B Phantom Miro Color Camera

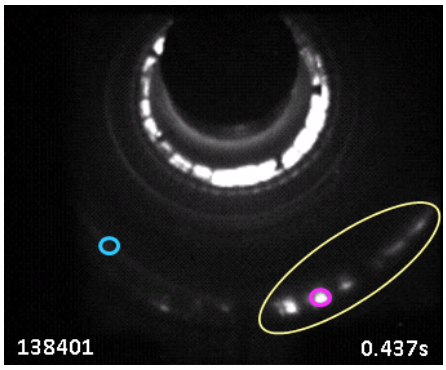

(b) Bay J Camera w/ RM90 Filter

FIG. 4: Hot streak (circled in yellow) created by SOL deposition of RF power on the outer divertor. A hot spot is marked in magenta, while a cooler spot with a similar level of plasma light is marked in cyan.

B. Divertor hot streak due to HHFW power loss to SOL

The high-harmonic fast wave (HHFW) antenna used to study radio frequency (RF) heating and current drive on NSTX is capable of delivering up to 6 MW of power to the plasma[17]. While the RF power would ideally be absorbed by the core of the confined plasma, a fraction of the power couples with the scrape-off layer (SOL) and strikes the outer divertor. Recent studies have shown that for $\sim$ 2 MW of RF power, several hundreds of kilowatts[18] can be lost to the SOL and deposited in small region of the outer divertor that is magnetically connected to the HHFW antenna. An increase in the heat flux in this region of up to a factor of six was observed in some shots[17], leading to a radially narrow area of heated tiles that extends approximately 90^o toroidally around the outer divertor. This hot streak provides a good test case for our proposed system's temperature measurement capabilities.

As shown in Figure 4, the hot streak can clearly be observed during RF operation by both a Phantom Miro color camera and the Phantom v7.3 camera with a 900 nm filter. In the Miro image (Figure 4a), bright fila-

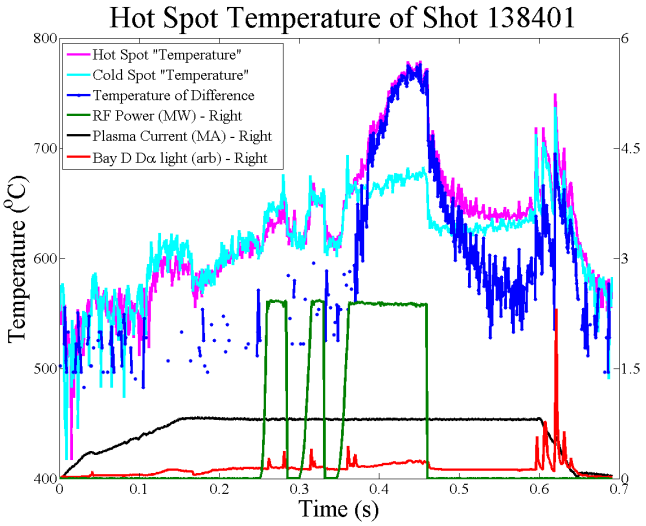

FIG. 5: The observed "temperature" in shot 138401 for the hot spot (magenta) and cold spot (cyan) marked in Figure 4b. The cold spot lies on the same field line as the hot spot, so both should have similar levels of plasma light. Blue shows the temperature measured using the difference in the hot spot and cold spots counts.

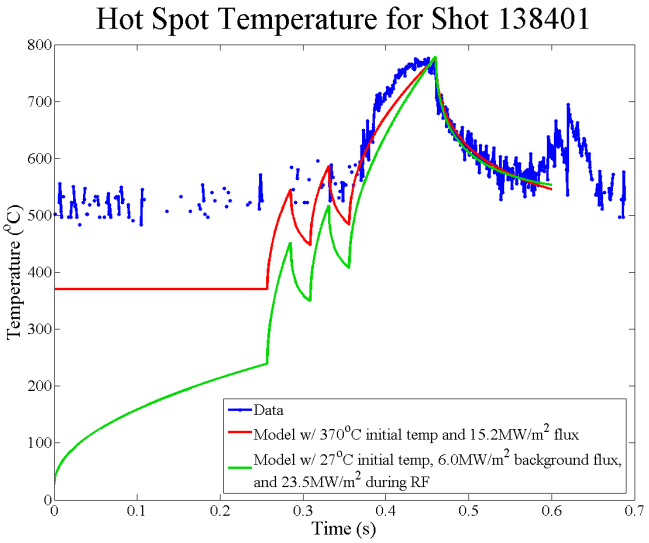

FIG. 6: Two theoretical fits to the temperature measured for shot 138401.

ments of plasma appear in the edge region aligned with the magnetic field during the RF operation; these heated SOL filaments magnetically link the hot streak to the HHFW antenna. The bright filaments can also be observed faintly in the NIR movies, passing through and extending beyond the hot streak. Unfortunately, the filaments are not readily visible in still images and are nearly invisible in Figure 4b. The hot streak is broken up into several discrete hot spots, possibly due to scales of lithium or other impurity films built up in those particular locations. Such scales have poor thermal contact with the bulk material, which can lead to locally higher surface temperatures.

Figure 5 shows a temperature analysis of shot 138401 using data from the Bay J Phantom v7.3 camera and a 900 nm filter. The temperature given by the average count inside the magenta circle (a hot spot) in Figure 4b and the temperature given by the average count inside the cyan circle (a "cold" spot) in Figure 4b are plotted. This cold spot lies along the same RF heated plasma filament as the hot spot; for lack of a better method, we use this cold spot to provide an approximate measure of the background plasma light found at the hot spot. This method is partially validated by the temperature curves of both spots lying on or near each other for much of the shot. Before the RF pulse, the ~ 600 ^{o}C temperature observed for both spots is consistent with the background equivalent temperature found in Figure 3c in the region outside the strike point. Therefore, we attribute this high initial temperature to background plasma light. During the long RF pulse beginning at $t \approx 0.350$ s (see the green curve in Figure 5), the hot and cold curves diverge with the hot spot temperature rising ~ 150 ^{o}C in 100 ms. This corresponds to about a hundred-fold increase in the number of counts observed between the hot and cold spots. The dark blue curve in Figure 5 shows the temperature given by the difference in the hot and cold spot counts, in an attempt to account for the plasma light background. Times where the hot spot count did not exceed the cold spot count by at least one standard deviation have been removed. While the peak temperature of the hot spot is largely unchanged by removing this background, the spurious initial high temperature of the divertor indicated by the non-adjusted counts is almost entirely removed. In addition, the observed temperature is drawn downward by ~ 100 ^{o}C both at the beginning of the long RF pulse and shortly after the pulse as the hot spot cools.

C. Modeling the thermal signature

To determine the how well this data matches a thermal signature, a simple 1D thermal code was made to model the temperature of a divertor tile in the presence of a heat flux. We assume the heat flux is incident on a one inch thick tile of ATJ graphite. We solve 1D diffusion equation, $\frac{\partial T}{\partial t} = \chi \frac{\partial^2 T}{\partial x^2}$, using the explicit Forward Time Centered Space (FTCS) discretization scheme. On the bottom side of the tile, we apply a zero flux boundary condition, while the top of the tile is subject to a piecewise constant flux. We assume a constant diffusivity, $\chi = 0.34$ cm^2/s, and conductivity, $\kappa = 0.94$ W/(cm K). These are the values for ATJ graphite at 600 ^{o}C. Variation of these parameters to their appropriate values at higher or lower temperature yielded negligibly different qualitative results.

We used two different flux profiles to fit our data. The

first assumes zero heat flux into the tile while the HHFW antenna is off and a constant flux during the RF pulses. We found that the temperature rise during RF for shot 138401 was well-fit by this model with an initial temperature of 370 ^{o}C and a 15.2 MW/m^2 heat flux, particularly in the decaying region after the RF is turned off (see the red curve in Figure 6). Analysis of data from the ORNL slow IR camera implied a heat flux roughly consistent with our measurements. That said, the initial starting temperature of 370 ^{o}C is far too high. Presumably, the divertor is near room temperature at the beginning of the shot. Thus, a second model was developed with a fixed initial temperature of 27 ^{o}C and a constant background heat flux into the tile while the RF is off. The green curve in Figure 6 shows our manual fit of this model to the data from shot 138401, with a background flux of 6.0 MW/m^2 without RF and a total flux of 23.5 MW/m^2 during the RF pulses. Again, we find that the data is fairly well-fit, though not quite as well as by the first model. Unfortunately, both the 6.0 MW/m^2 without RF and 23.5 MW/m^2 with RF are somewhat higher than those measured by the ORNL slow IR camera.

While neither model used provides both a reasonable heat flux and initial temperature, this does not necessarily imply that the observed bright spot has a nonthermal source. Rather, as previously noted, it is likely that these hot spots occur where scales of lithium and other impurities have built up. Such scales and surface films can significant complicate the analysis of thermal signals. Since the surface temperature as a function of time of a semi-infinite solid in the presence of a constant flux[19] is $T(t) = \frac{2F}{\kappa}\sqrt{\frac{\chi t}{\pi}}$, a decrease in the conductivity or increase in the diffusivity would decrease the flux measured in the second model. Determining the thermal properties of impurity scales and films is beyond the scope of the present paper. Nevertheless, the models above indicate that the data is at least consistent with a thermal rise during an extended RF pulse, allowing us to be reasonably certain that we are observing thermal emission.

IV. CONCLUSION

High-speed cameras sensitive mainly to visible light have been installed onto NSTX to observe the divertor region. A benchtop calibration of these cameras with near-infrared filters demonstrated the system's ability to be used for IR thermography. *In situ* cross-calibration with an ORNL fast-IR, dual-band camera showed that plasma background light produces a background equivalent temperature between 500 ^{o}C and 700 ^{o}C. Temperatures belows these values cannot be measured during a shot with the current system in the NSTX divertor environment. We were able, however, to measure temperatures in excess of 700 ^{o}C in RF-heated hot spots with this system.

A main objective of future work on this system will be the determination and/or elimination of the plasma light background. Line emission filters could be used to measure the amount of background light, allowing for its subtraction from the NIR signal. Alternatively, narrow band-pass filters in a frequency region relatively free of emission lines could be used to isolate thermal emission light. An improved thermal model that includes the effects of impurity buildups on the tiles would allow for more extensive comparisons to the ORNL IR measurements. Furthermore, future *in situ* calibrations of our system could allow us to account for changes that occur over the course of a run cycle (e.g., non-ideal emissivities and decreased transmittance due to window coatings). Lastly, our systems high-speed capabilities were not put to full use. Future studies on transient heating throughout the divertor due to ELMs and disruptions may be possible with our system.

ACKNOWLEDGMENTS

This work was supported by Department of Energy (DOE) contract number DE-AC02-09CH11466 and, in part, by an award from the DOE Office of Science Graduate Fellowship Program (DOE SCGF). The DOE SCGF Program was made possible in part by the American Recovery and Reinvestment Act of 2009. The DOE SCGF program is administered by the Oak Ridge Institute for Science and Education for the DOE. ORISE is managed by Oak Ridge Associated Universities (ORAU) under DOE contract number DE-AC05-06OR23100. All opinions expressed in this paper are the author's and do not necessarily reflect the policies and views of DOE, ORAU, or ORISE.

Thank you to the entire NSTX team for their support in conducting these experiments.

[1] A. Loarte *et al.*, Nucl. Fusion **47** (2007).
[2] R. Tivey *et al.*, Fusion Engineering and Design **55** (2001).
[3] A. Kallenbach *et al.*, Plasma Phys. Control. Fusion **52** (2010).
[4] A. Kallenbach *et al.*, Nucl. Fusion **48** (2008).
[5] G. Arnoux *et al.*, Journal of Nuclear Materials **390-391** (2009).
[6] T. Eich *et al.*, Journal of Nuclear Materials **313-316** (2003).
[7] E. Gauthier *et al.*, Journal of Nuclear Materials **363-365** (2007).
[8] J. van Rooij *et al.*, Journal of Nuclear Materials **390-391** (2009).
[9] G. DeTemmerman *et al.*, Plasma Phys. Control. Fusion **52** (2010).
[10] J. Marki *et al.*, Journal of Nuclear Materials **390-391** (2009).
[11] J. Terry *et al.*, Rev. Sci. Instrum **81**.
[12] R. Reichle *et al.*, Rev. Sci. Instrum **81**.
[13] D. Mastrovito *et al.*, Rev. Sci. Instrum **74** (2003).
[14] J. Ahn *et al.*, Rev. Sci. Instrum **81** (2010).
[15] A. McLean *et al.*, "Update on high-speed infrared imaging of the NSTX divertor." Presented at NSTX Weekly Physics Meeting (2010).
[16] V. Soukhanovskii *et al.*, Rev. Sci. Instrum **79**.
[17] G. Taylor *et al.*, Phys. Plasmas **17** (2010).
[18] J. Hosea *et al.*, "High harmonic fast wave heating studies for L and H mode NSTX plasmas," Presented at the 51st APS-DPP Meeting (2009).
[19] H. Carslaw and J. Jaeger, *Conduction of Heat in Solids.*, 2nd ed. (Oxford University Press., 1959).

The Princeton Plasma Physics Laboratory is operated
by Princeton University under contract
with the U.S. Department of Energy.

Information Services
Princeton Plasma Physics Laboratory
P.O. Box 451
Princeton, NJ 08543

Phone: 609-243-2245
Fax: 609-243-2751
e-mail: pppl_info@pppl.gov
Internet Address: http://www.pppl.gov